General Disclaimer

One or more of the Following Statements may affect this Document

- This document has been reproduced from the best copy furnished by the organizational source. It is being released in the interest of making available as much information as possible.

- This document may contain data, which exceeds the sheet parameters. It was furnished in this condition by the organizational source and is the best copy available.

- This document may contain tone-on-tone or color graphs, charts and/or pictures, which have been reproduced in black and white.

- This document is paginated as submitted by the original source.

- Portions of this document are not fully legible due to the historical nature of some of the material. However, it is the best reproduction available from the original submission.

NASA TECHNICAL MEMORANDUM

NASA TM X- 73,117

NASA TM X-73,117

LASER VELOCIMETRY APPLIED TO TRANSONIC AND SUPERSONIC AERODYNAMICS

D. A. Johnson, W. D. Bachalo, and D. Moddaress

Ames Research Center
Moffett Field, California 94035

March 1976

1. Report No.	2. Government Accession No.	3. Recipient's Catalog No.
NASA TM X-73,117		

4. Title and Subtitle	5. Report Date
LASER VELOCIMETRY APPLIED TO TRANSONIC AND SUPERSONIC AERODYNAMICS	6. Performing Organization Code

7. Author(s)	8. Performing Organization Report No.
D. A. Johnson, W. D. Bachalo,* and D. Moddaress*	A-6510
	10. Work Unit No. 505-06-43

9. Performing Organization Name and Address	11. Contract or Grant No.
NASA Ames Research Center Moffett Field, CA 94035	
	13. Type of Report and Period Covered
12. Sponsoring Agency Name and Address	Technical Memorandum
National Aeronautics and Space Administration Washington, D. C. 20546	14. Sponsoring Agency Code

15. Supplementary Notes

*Resident Research Associate, National Research Council

16. Abstract

As a further demonstration of the capabilities of laser velocimetry in compressible aerodynamics, measurements obtained in a Mach 2.9 separated turbulent boundary layer and in the transonic flow past a two-dimensional airfoil section are presented and compared to data realized by conventional techniques. In the separated-flow study, the comparisons were made against pitot-static pressure data. Agreement in mean velocities were realized where the pressure measurements could be considered reliable; however, in regions of instantaneous reverse velocities, the laser results were found to be consistent with the physics of the flow whereas the pressure data were not. The laser data obtained in regions of extremely high turbulence suggest that "velocity biasing" does not occur if the particle occurrence rate is low relative to the turbulent fluctuation rate. Streamwise turbulence intensities are also presented, although, no such similar data are available for comparison. In the transonic airfoil study, velocity measurements obtained immediately outside the upper surface boundary layer of a 6-inch chord NACA 64A010 airfoil are compared to edge velocities inferred from surface pressure measurements. For free-stream Mach numbers of 0.6 and 0.8, the agreement in results was very good. "Dual scatter" optical arrangements in conjunction with a single particle, counter-type signal processor were employed in these investigations. Half-micron-diameter polystyrene spheres and naturally occurring condensed oil vapor acted as light scatterers in the two respective flows. Bragg-cell frequency shifting was utilized in the separated flow study.

17. Key Words (Suggested by Author(s))	18. Distribution Statement
Laser velocimeter Shock-induced separation Transonic 2-D airfoil Supersonic and transonic wind tunnels	Unlimited STAR Category - 35

19. Security Classif. (of this report)	20. Security Classif. (of this page)	21. No. of Pages	22. Price*
Unclassified	Unclassified	13	$3.25

*For sale by the National Technical Information Service, Springfield, Virginia 22161

LASER VELOCIMETRY APPLIED TO TRANSONIC AND SUPERSONIC AERODYNAMICS

D. A. Johnson,* W. D. Bachalo,† and D. Mcddaress†
Ames Research Center, NASA
Moffett Field, CA 94035, U.S.A.

SUMMARY

As a further demonstration of the capabilities of laser velocimetry in compressible aerodynamics, measurements obtained in a Mach 2.9 separated turbulent boundary layer and in the transonic flow past a two-dimensional airfoil section are presented and compared to data realized by conventional techniques. In the separated-flow study, the comparisons were made against pitot-static pressure data. Agreement in mean velocities were realized where the pressure measurements could be considered reliable; however, in regions of instantaneous reverse velocities, the laser results were found to be consistent with the physics of the flow whereas the pressure data were not. The laser data obtained in regions of extremely high turbulence suggest that "velocity biasing" does not occur if the particle occurrence rate is low relative to the turbulent fluctuation rate. Streamwise turbulence intensities are also presented, although, no such similar data are available for comparison. In the transonic airfoil study, velocity measurements obtained immediately outside the upper surface boundary layer of a 6-inch chord NACA 64A010 airfoil are compared to edge velocities inferred from surface pressure measurements. For free-stream Mach numbers of 0.6 and 0.8, the agreement in results was very good. "Dual scatter" optical arrangements in conjunction with a single particle, counter-type signal processor were employed in these investigations. Half-micron-diameter polystyrene spheres and naturally occurring condensed oil vapor acted as light scatterers in the two respective flows. Bragg-cell frequency shifting was utilized in the separated flow study.

NOMENCLATURE

c	chord length of airfoil	α	angle of attack
d_p	particle diameter	α_o	optical size parameter, $\frac{\pi d_p}{\lambda}$
$e(t)$	photodetector voltage	δ	boundary-layer thickness
f_B	Bragg-cell frequency shift	θ	angle between incident beams
f_{3dB}	frequency response (half-power point)	λ	wave length of light
$g(r_o,\vec{V})$	envelope function for single particle burst	μ	viscosity
I_o	local light intensity	ρ_p	particle density
m	particle index of refraction	ρ	nondimensional optical parameter, $2\alpha_o(m - 1)$
M	Mach number	σ	standard deviation
N	total number of realizations	τ_c	particle relaxation time (1/e point)
P_{sca}	total scattered light	τ_o	time between zero crossings
Q_{sca}	efficiency factor for scattering	ϕ	phase angle
r_o	particle position at $t = 0$	Ω	Bragg angle
R_e	Reynolds number	$\langle\rangle$	rms of quantity
t	time		
T	time long (relative to turbulent fluctuations)		
u	streamwise velocity component		
$u_\perp$	velocity component perpendicular to fringes		
$\vec{V}$	velocity vector		
v_f	fringe velocity		
x	streamwise coordinate		
x_c	particle response distance (1/e point)		
x_f	fringe spacing		
y	coordinate normal to surface		

Subscripts

g	gas
h	high pass filtered
i	individual realization
p	particle
t	stagnation conditions
∞	freestream conditions

Superscripts

$( )'$	fluctuation quantity
$(\bar{})$	time-averaged quantity

INTRODUCTION

Laser velocimetry has the potential of making a tremendous impact in the area of compressible aerodynamics. In principle, this technique can be used in compressible flows to obtain very localized velocity (speed and flow direction) and turbulence information, which would be impossible to obtain with any other measurement technique. Obviously important is its nonintrusive property, but also important is the straightforward signal interpretation it affords in variable property flows. For example, in the study of compressible turbulent flows, the Reynolds normal and shear stresses can be measured without the signal interpretation difficulties involved with hot-wire anemometry. In regions of turbulent separation forward and reverse instantaneous velocities can easily be distinguished through frequency shifting techniques. Such directional information is not achievable with other existing techniques. Also, since it has truly linear response, no inaccuracies need result when the fluctuations are large compared to the mean value.

The measurement of local flow directions has always presented a problem, but, with the laser velocimeter, this measurement is straightforward, especially for two-dimensional flows. In regions of inviscid

*Research Scientist.
†Resident Research Associate, National Research Council.

flow where the total pressure is constant, such as the flow about airfoil sections, pitot tube measurements provide no information. Information can be obtained from static pressure probe measurements, but these are suspect, especially in regions of flow angularity. The laser velocimeter can provide a complete definition of the inviscid flow, including the surface pressure distributions in the absence of boundary-layer separation. Even if shock waves are present, the inviscid flow can still be completely specified, since changes in total pressure can be determined from the measured velocity vectors.

As with any measurement technique, the laser velocimeter, however, is not without its shortcomings. The requirement of minute particles for light scattering, which are sufficiently small to track the fluid motion, and the requirement that the scattered light levels from these particles be sufficient to achieve processable signals make the application of laser velocimetry in high-speed wind tunnels especially difficult.

In most compressible flows of practical importance, there occur extremely large velocity gradients that impose severe particle trackability requirements. Thus, in general, the particles to be used for light scattering must be much smaller than those permissable for use in low-speed applications. These smaller particles scatter less light, thereby making their detection more difficult. Light detection is further complicated at high velocities, since the total light scattered by a given size of particle varies inversely with residence time in the sensing volume.

Despite these difficulties, several investigators have demonstrated (through comparisons with results obtained from conventional instrumentation) the technique's ability to provide accurate localized velocity information in high-speed wind tunnels. Favorable mean velocity comparisons with pitot-tube measurements have been obtained (Refs. 1-4) for turbulent supersonic boundary layers (zero pressure gradient). Good agreement has also been obtained with hot-wire anemometer measurements of the Reynolds normal and shear stresses for an undisturbed turbulent supersonic boundary layer (Ref. 5) and for a shock wave/turbulent boundary-layer interaction (Ref. 6). The Reynolds normal and shear stress results of Ref. 3 were found to agree well with those of Ref. 5, lending even more credibility to both sets of data. Interestingly, in Ref. 3, relatively large (5-μm diam) particles were shown to give reliable results; an indication that the particle trackability requirements are not severe for equilibrium supersonic boundary layers.

Laser velocimeter results have also been reported (Ref. 7) for the supersonic flow past a 10° cone, and shown to be in good agreement with theory. A very limited number of laser velocimeter measurements have been presented for a transonic separated boundary layer on a two-dimensional bump (Ref. 8). However, particle lag was so dominant in that study that the mode value, rather than the first moment, of the histograms had to be used to approximate the fluid mean velocity.

The present paper describes the further application of laser velocimetry to two flows which are of extreme interest in compressible aerodynamics and which impose severe requirements on the light-scattering particles' ability to track the fluid motion. They are (i) the shock-induced separation of a supersonic turbulent boundary layer and (ii) the transonic flow past an airfoil section. The particle response requirements of these flows are representative of those to be expected in practical internal and external aerodynamic flow problems. In the former flow, to demonstrate the accuracies of the laser technique, boundary-layer profile data obtained by laser velocimetry are compared to pitot-static pressure probe results obtained for the same flow conditions. Along with these data, the streamwise turbulence intensities are also presented. Surface pressure data were used in the transonic airfoil study to verify the velocimeter's measurement capabilities. The investigations were conducted in the Ames 8- by 8-Inch Supersonic Wind Tunnel and the Ames 2- by 2-Foot Transonic Wind Tunnel, respectively.

LASER VELOCIMETRY

Velocity Detection

As in Refs. 2, 5, and 6, the "fringe" or "dual scatter" optical arrangement was employed in the current investigations. Of the several conceived optical arrangements for laser velocimetry, this configuration has become the most popular for air flow applications where particle concentrations tend to be low, and it is treated quite thoroughly in the literature (e.g., Refs. 9-11). Unlike other arrangements, it affords large, solid-angle light collection without any associated signal broadening or coherence problems. This property is extremely important when velocity measurements are to be made from small individual light scatterers that may be submicron in size.

The principle of operation can be visualized as follows: Two coherent, parallel laser beams with Gaussian intensity distributions are brought to focus at a common point with a positive lens, thus forming a set of intensity fringes, as depicted in Fig. 1. These planar fringes are equally spaced at a distance $x_f = \lambda/(2 \sin \theta/2)$. They are parallel to the bisector of the two incident beams and perpendicular to the plane formed by the two incident beams. As a particle that is small with respect to the fringe spacing passes through this field of spatially varying light intensity, the amount of light scattered by the particle changes in proportion to the light intensity incident upon it. Some of this scattered light is collected and transmitted to a photodetector, which produces an electrical signal that represents the intensity of the fringe pattern, but in time rather than in space. The signal burst produced at the photodetector by an individual particle crossing the sensing volume has the form (Ref. 11)

$$e(t) = \frac{1}{2} e^{-g(r_o,\vec{V})t^2}\left(1 - \cos \frac{2\pi u_\perp}{x_f} t\right)$$

where the envelope function g depends on the trajectory of the particle passing through the sensing volume. Passing this signal through a high-pass filter produces a signal given by

$$e_h(t) = \frac{1}{2} e^{-g(r_o,\vec{V})t^2} \cos \frac{2\pi u_\perp}{x_f} t$$

that is symmetric with respect to zero and which crosses zero at fixed time intervals of

$$\tau_o = \frac{1}{2} \frac{x_f}{u_\perp}$$

Notice that this time depends only on (i) the velocity component that is perpendicular to the interference fringes $u_\perp$, and (ii) the known fringe spacing. By orienting the fringes appropriately, any desired velocity component can be sensed.

To accomplish the measurement of τ_0, a signal processor similar to that described in Ref. 12 was employed. This zero-crossing counter measures the time for 16 zero crossings (8 fringe crossings) to improve the time resolution. A check on whether the signals have the necessary periodicity is also performed by comparing the time for five fringe crossings to that for eight.

From the individual signal bursts, nearly instantaneous samples of the local velocity component perpendicular to the fringes are realized. By acquiring a large number of these velocity samples, the probability density function (pdf) of the velocity component under observation is obtained, provided the sampling is random. Estimates of the first and second moments of the velocity component can be obtained from a fewer number of samples by using the statistical estimators

$$\bar{u} = \frac{1}{N} \sum_{i=1}^{N} u_i$$

and

$$\langle u' \rangle = (\overline{u'^2})^{1/2} = \frac{1}{N} \sum_{i=1}^{N} (u_i - \bar{u})^2$$

In the present studies, histograms were developed by transferring the counter output to a pulse height analyzer from which using the above equations, $\bar{u}$ and $\langle u' \rangle$ were calculated. The number of realizations needed to obtain accurate estimates varied considerably between the two studies. In the airfoil study, wherein the turbulence levels were very low, only a few hundred samples were necessary. Typically, two thousand were used, many more than required. In the separated flow study, due to the high turbulence levels, much larger samples were needed. In the regions of high turbulence, 10 to 20 thousand realizations were obtained for each calculation. The effects of spurious readings were reduced by ignoring velocity readings whose relative occurrences were a factor of 50 less than the most likely reading. For a Gaussian distribution, this is equivalent to ignoring points beyond $\pm 2.8\sigma$ of the mean.

When the two incident beams in Fig. 1 are of the same frequency, the intensity fringes are stationary in space. Thus, identical signals are produced by either forward or backward traveling particles. This ambiguity can be alleviated by producing a slight frequency shift in one of the beams (Refs. 13, 14). In so doing, the phase difference between the two beams changes at a constant rate given by

$$\frac{d\phi}{dt} = 2\pi f_B$$

where f_B is the frequency shift. In the time given by $1/f_B$, the phase undergoes a change of 2π radians, which causes a displacement in the intensity fringes equal to the fringe spacing x_f. Since the time rate of change in phase is constant, the fringes travel at a constant velocity, given by $v_f = x_f f_B$. With the fringe intensity pattern traveling at a velocity v_f, a stationary particle in the probe volume produces a signal with period $1/f_B$. A particle traveling in the direction of the fringes produces a signal with a longer period and, conversely, a particle traveling in the opposite direction produces a signal with a shorter period. Thus, forward and reverse velocities can be distinguished.

While this capability is obviously important in the detection of reversing flows, it should also be used with zero-crossing counter techniques in highly turbulent flows, because of the requirement for a minimum of 8 fringe crossings. Otherwise, in regions of high turbulence, regardless of the orientation of the fringes, some particles will pass through the sensing volume, which, because of practical limitations, contains a finite number of fringes, such that less than eight fringes are crossed. The measurement system in this case accumulates a biased sample. For this reason and for resolution of reversing velocities, a frequency offset produced by a solid crystal Bragg cell was used in the investigation of the shock-induced separated turbulent boundary-layer flow.

Particle Response and Light Scattering

For the realization of accurate laser velocimeter measurements, particle lag effects due to the particles' inertia must be negligible. To insure this, the particles must be sufficiently small. This can be seen from the equation given below which describes the particle response to a discontinuous change in gas velocity.

$$\frac{du_p}{dt} = \frac{18\mu_g}{\rho_p d_p^2} (u_g - u_p)$$

In the above equation, the drag coefficient for the spherical particle has been approximated by Stokes' value of 24/Re. The solution of this equation has the exponential decay form in which the time constant τ_c (i.e., the 1/e point) is given by

$$\tau_c = \frac{\rho_p d_p^2}{18\mu_g}$$

Thus, subject to the accuracy of the Stokes' drag law (Ref. 15), the time constant is proportional to the square of the particle diameter for fixed fluid properties and particle density. Analagous to the 3-dB frequency response quoted for hot-wire anemometry, but in the moving reference frame of the particle, the particle response is given by

$$f_{3dB} = \frac{1}{2\pi\tau_c}$$

If we assume the step change in velocity to be small, the response distance can be expressed as

$$x_c = u_g \tau_c$$

Values for τ_c, f_{3dB}, and x_c are given in Table 1 for different sizes of particles with a specific gravity of unity in a Mach 3 flow with a 293°K stagnation temperature. For lower Mach numbers, these values improve because of the decrease in u_g and the increase in μ_g (e.g., μ_g is two and half times larger at ambient temperature conditions).

From a particle dynamics standpoint, the smaller the particle, the better; but for a given laser velocimeter system, there will be a minimum particle size for which accurate measurements can be obtained. This sensitivity is determined by how much scattered light can be collected from a given size of particle, by the amount of background laser radiation, and by the performance of the signal processing electronics. From Mie scattering theory, the amount of scattered light that can be collected depends on (i) the light intensity achieved at the sensing volume, which is governed by the total laser power and degree of focusing, (ii) the

solid angle over which the light is collected, (iii) the direction from which the light is collected, (iv) the index of refraction of the particle, and (v) the optical size parameter $\alpha_o = \pi d_p/\lambda$. The amount of background laser light plays a significant role, since it contributes to photodetector shot-noise.

Experience has shown that measurements can be quite easily obtained, at least for low speeds, from micron sized particles with relatively low-power lasers. However, when the particle size gets substantially less than 1 μm, detection becomes exceedingly difficult. The reason for this can be seen by observing how the efficiency factor for scattering Q_{sca}, which is related to the total scattered light by

$$P_{sca} = Q_{sca} \cdot \frac{\pi}{4} d_p^2 \cdot I_o$$

depends on the nondimensional parameter $\rho = 2\alpha_o(m - 1)$ given in Ref. 16. As seen in Fig. 2, the efficiency factor has a peak value at $\rho = 4$ and then falls off rapidly for smaller values. This value of ρ corresponds to a particle diameter of 0.55 μm for $\lambda = 514.5$ nm.

Interestingly, due to this rapid decrease in Q_{sca} and the trend for more symmetric scattering as ρ decreases, the difference in minimum detectable particle size for forward- and back-scatter is small if sufficient laser power and solid-angle light collection are used. For example, at an index of refraction of 1.55 the intensity of light scattered in the backward direction for a 0.5-μm particle is the same as in the forward direction for a 0.25-μm-diam particle. A 1-μm-diam particle in back-scatter gives signals equivalent to a 0.4-μm particle in forward-scatter.

In the previous investigations in the 8-inch supersonic facility (Refs. 2, 5, and 6) only the naturally occurring particles were used for light scattering. This was because conventional aerosol generators at that time produced particles larger than existed naturally in the flow. Recently, aerosol research, in support of laser velocimetry, has progressed to the point where submicron particles can be reliably generated (Ref. 17). The aerosol used in the shock-induced separation study was produced by atomizing an aqueous solution containing uniformly sized polystyrene spheres. A particle diameter of 0.5 μm was selected as a compromise between particle response and light-scattering ability.

In the study performed in the transonic facility, the sparsity of particles observed in the supersonic tunnel did not exist. In this closed return tunnel, lubricant oil from the drive system vaporizes and then recondenses in the tunnel nozzle to produce particles of sufficient numbers for the laser velocimeter. Based on shock response measurements, these oil droplets are estimated to have a 1-μm-diam, which, at transonic conditions, give a response nearly equivalent to a 0.5-μm particle at Mach 3 conditions.

Velocity Biasing

As with any attempted localized measurement, the sensing volume must be small compared to the scale of the flow field. If not, spatial and time averaging can occur. Not only can this condition limit the resolution of the flow, but it can also cause measurement errors. The laser velocimeter is especially sensitive to spatial velocity variations, since the particle crossing rate is a function of the mean velocity. To avoid these problems, the probe volume must be sufficiently small such that the changes in a particle's velocity as it passes through the probe volume are negligible. Also, the variation in mean velocity across the probe volume must be small compared to the mean velocity being measured. In the measurements reported herein, these requirements were believed to have been met. Off-axis light collection was used to improve resolution in the cross-stream direction.

An insufficient number of fringe crossings in highly turbulent flows was discussed previously as a source of measurement errors when applying zero-crossing counter techniques. It has also been proposed (Ref. 18) that the occurrences of particle crossings are not random in a turbulent flow in that higher velocity particles have a higher probability of being sensed, hence a biased measurement is obtained. In Ref. 18, this biasing was concluded to be independent of the sampling rate. In another study of this subject (Ref. 19), it was argued that the velocity bias must depend on the rate at which the particle crossings occur relative to the turbulent frequencies; that is, if the particle occurrence rate is greater than the turbulence frequencies, the conclusions of Ref. 18 are valid, but, if the particle occurrence rate is much less than the turbulence frequencies, no biasing occurs. An argument which supports the conclusions of Ref. 19 is presented herein.

Consider a flow facility (see Fig. 3) where particles are released from the nonturbulent settling chamber into a turbulent flow in the test section, and then discharged from the flow facility. Due to the turbulence, each particle will follow some random path as do the fluid elements (here we are assuming negligible particle lag effects). Since a particle must travel from the settling chamber to the exit of the flow facility, its chances of intercepting the probe volume, δV, is dependent only on its initial position in the settling chamber. If a particle does intercept the probe volume, its velocity should only depend on the probability density function of the velocity vector at δV. The question arises, however, whether the rate of occurrence of these particle crossings is independent of the local instantaneous velocity. If it is not, then biasing can occur. To simplify the analysis of this aspect of the problem, consider a one-dimensional time-dependent problem: an infinite transparent rod which contains particles equally spaced along its length and which is given a random motion, u(t) (Fig. 4a). At a fixed station, A-A, the time between particle crossings Δt, is given implicitly by the intergral relationship

$$\int^{\Delta t} u(t)dt = \Delta x$$

where Δx, the distance between particles, is fixed by the definition of the problem. Now for very short Δt's, u(t) can be considered constant during Δt_i, and the time between particle arrivals is given by

$$\Delta t_i = \frac{\Delta x}{u(t)}$$

In this case, the rate of particle arrivals is seen to depend on the instantaneous velocity (Fig. 4b). Now consider the case where the particles are sparse. Then Δt is long compared to the rate of change in velocity and the following becomes true:

$$\int^{\Delta t} u(t)dt = \Delta t\left[\frac{1}{\Delta t}\int^{\Delta t} u(t)dt\right] = \Delta t\left[\frac{1}{T}\int^{T} u(t)dt\right]$$

Hence,

$$\Delta t = \frac{\Delta x}{\bar{u}}$$

Since $\bar{u}$ is a constant (i.e., the flow is stationary), Δt depends only on Δx, which, for this problem, is a constant (Fig. 4c). In the more general case, where the Δx's are randomly distributed, so also will Δt be random and independent of the instantaneous velocity; the conditions necessary for unbiased sampling.

In the present investigation, the calculations of mean and rms velocities were made assuming that the sampling was random and indeperdent of the instantaneous velocity (i.e., no velocity bias corrections were applied). This assumption was believed justified, since the data acquisition rate never exceeded 500 samples/sec. In the results section, the validity of this assumption is further discussed.

EXPERIMENTAL APPARATUS

Shock-Induced Separation

A full-span wedge set at an angle of 13° with respect to the oncoming flow (see Fig. 5) was used to generate the shock-induced separated flow. The shock wave produced by this turn in the flow impinges on the upper nozzle wall boundary layer of the tunnel, producing separation. Free-stream conditions were $M_\infty = 2.9$ and a unit Reynolds number of $5.7\times10^7 m^{-1}$. The initial boundary-layer thickness δ was approximately 2 cm and the pressure rise produced by the interaction was sufficiently strong to cause a separation bubble nearly 6-cm long. This flow had been previously investigated, wherein pitot and static pressure data were obtained (Ref. 20).

The laser velocimeter system and its orientation to the supersonic tunnel is shown in a plan view in Fig. 6. It is a single-velocity component system with off-axis, forward-scatter light collection. The incoming beams were aligned perpendicular to the tunnel centerline and parallel to the surface of the upper tunnel wall. To achieve a frequency shift, a solid crystal Bragg cell was used; this also accomplished the splitting of the original laser beam into two equal intensity beams. The frequency shifted and unshifted beams were brought parallel to each other by an optical cube that had been designed to compensate for the Bragg angle Ω. The frequency offset of this cell was 40 MHz. The angle θ between the two incident beams, ranged between about 1.5° and 0.5°. The smaller values of θ were required in regions of very high turbulence to keep the excursions in frequency within the usable bandwidth of the zero-crossing counter. Before the signal was processed, electronic mixing of the photodetector output with a double balanced diode mixer was employed, either to achieve the desired number of fringe crossings or to reduce the signal frequencies to values below the upper frequency limit of the counter (50 MHz).

The effective sensing volume of the velocimeter was approximately a cylinder with a 0.3-mm (0.015δ) diam and a 1.5-mm length whose axis was in the cross-stream direction. Precise translation in the direction normal to the tunnel wall surface was accomplished with stepping-motor-driven lead screws. A laser output level of 1 watt at the 514.5-nm wavelength was typical, and the F number for light collection was about 4.

The light scattering particles were produced from a liquid suspension containing polystyrene spheres. A Laskin-type nozzle arrangement was used to atomize this suspension, then drying was accomplished by mixing the aerosol with dry air. The aqueous solution of these monodisperse polystyrene spheres, as received from the manufacturer, was diluted heavily with water so that there was a low probability that the liquid droplets produced by the Laskin nozzle would contain more than one of these solid spheres and hence a low probability that doublets or higher multiples would form (Ref. 17). The aerosol of polystyrene spheres produced in this manner were injected into the top of the plenum chamber of the tunnel through a stainless steel tube. The depth of penetration of this vertical tube into the plenum chamber was variable. Complete drying of the aerosol was confirmed by first operating the particle generator with pure water and observing that no single particle signals were detected with the laser velocimeter.

Transonic Airfoil Study

In the study of the flow over a two-dimensional airfoil section, a 6-inch chord NACA 64A010 airfoil was selected for which conventionally obtained surface pressure distribution data from the same facility were available. The laser velocimeter system used in the investigation had been designed specifically for application in the Ames 2- by 2-Foot Transonic Wind Tunnel. A schematic of the laser installation is shown in Fig. 7. The test section of the tunnel, as with most transonic facilities, is enclosed by a large plenum chamber as shown in the schematic. To facilitate probing as much of the test section as possible and to reduce the range requirements of the velocimeter, part of the transmitting optics and all of the collecting optics were installed within the tunnel plenum area. A photograph of this portion of the system is shown in Fig. 8 (the mirrors allow the laser beams to be positioned wherever desired without displacing the laser). Three-dimensional translation is accomplished by stepping motors controlled outside the plenum area. The system is based on off-axis, back-scatter light collection. Although only a single component sensitivity was used in the present study, the collecting optics are designed for a two-component (dual color) capability.

The sensing volume for this system was approximately a cylinder, 0.4-mm diam and 2-mm long. The angle θ, between the two incident beams, was about 1.5°, and the light collection F number was 6. For this system, an Argon-ion laser capable of delivering over 6 watts in the 514.5 nm wavelength was used.

RESULTS

Shock-Induced Separation

To verify that the particles used for light scattering were in fact 0.5-μm diam, measurements were first taken across the incident oblique shock wave to evaluate particle response. The results of these measurements, with and without artificial seeding, are shown in Fig. 9. The rate at which particles crossed the sensing volume with artificial seeding was nominally 50 times greater than without, so the presence of the naturally occurring particles had a negligible effect on the results obtained during seeding. As evident from Fig. 9, the polystyrene spheres were able to respond nearly four times faster than the naturally occurring particles. Slight fluctuations in the shock wave's location complicated the determination of the response curves. However, since the shock wave spent more time at the two extrema, double peaked histograms resulted from which a relaxation curve could be inferred. The relaxation distances for the seeded and unseeded particles were in good agreement with those predicted from Stokes' drag law for 0.5-μm and 1-μm diam particles, respectively.

Figure 10 depicts the flow field, with the incident shock, induced shock, expansion fan, and reflected induced shock. In addition to the pressure measurements, the separation and reattachment points of the turbulent boundary layer were determined from oil-flow visualization in Ref. 20. Figure 10 also depicts these locations and the streamwise stations for which laser velocimeter data are presented.

Since comparisons are to be made with mean velocity determinations realized from local total and static pressure measurements, the accuracies of this long-used technique must be considered. In regions where the mean flow is parallel to the axes of these probes, historically this technique has been considered accurate to within a few percent, provided that backflow does not occur. However, when the probes are not aligned with the flow and the flow direction is unknown, several problems arise. First, the pressure measurements actually give the magnitude of the velocity vector and, if the mean flow direction is not known, the magnitude of the velocity component in a desired direction is not resolvable. Secondly, measurement errors in static pressure can result if the static probe is only slightly misaligned with the oncoming flow.

In the upstream region of the interaction where the outer flow is parallel to the wall, the pressure data should be valid, provided there are no reverse velocities. In Fig. 11, the mean velocities obtained with the laser velocimeter and pressure probes far upstream of the interaction (Fig. 11a) and near the separation point (Fig. 11b) are compared. The two sets of data are noted to be in good agreement, except near the wall at the separation point. At this location, the laser velocimeter indicated there was backflow a high percentage of the time, which accounts for the over prediction in mean velocity with the pressure probes. The streamwise turbulence intensities relative to the free-stream velocity, u_∞, as determined with the laser velocimeter, are also presented in Fig. 11. Notice the large change in turbulence levels between the two streamwise stations.

Profiles obtained in the separated flow region and near boundary-layer reattachment are presented in Fig. 12. At these two stations, the measurements are seen to agree only in the middle portion of the boundary layer. The disagreement in boundary-layer edge velocities is believed to be due to flow angularity outside the boundary layer, since, further downstream, both measurement techniques converge to the same edge velocity of 500 m/sec. Near the wall, the laser velocimeter data show a behavior consistent with the physics of the flow; smooth profiles with negative mean velocities in the separated region and non-negative mean velocities at reattachment. The pressure-probe data are obviously in error near the wall. Even if they were faced in the backward direction in the separated flow region, errors would be expected, as noted at the separation and reattachment points.

At the three downstream stations, notice that the turbulence intensities relative to the local mean velocity, $\langle u' \rangle / \bar{u}$, in the middle portion of the boundary layer were 50% or higher, yet agreement in the laser and pressure measurements was obtained in these regions. The one-dimensional velocity bias correction proposed in Ref. 18 would have predicted the laser data to be 25% high for this turbulence level. The data are in support of the argument that "velocity biasing" does not occur if the sampling rate is low compared to the turbulent fluctuation rate. A verification that the time between particle arrivals was not correlated with the streamwise velocity was made by sampling the "sample and hold" output of the counter at a fixed rate about 100 times faster than the mean data rate, rather than using a data-ready pulse to initiate a sample. The resulting histogram showed no deviations from the conventionally obtained histogram, thereby indicating no correlation between u_i and Δt_i.

Overall, it is believed safe to conclude that the laser velocimeter measurements presented herein are more accurate than previously attempted measurements in turbulent separated flows using physical probes.

Transonic Airfoil Section

In principle, airfoil surface pressures (in the absence of boundary-layer separation) can be determined by measuring the local static pressure just outside the airfoil boundary layer; the reason for this is that the static pressure is very nearly constant across the thin boundary layer. If the flow is isentropic, this pressure can be realized solely from a localized velocity measurement provided by the laser velocimeter. The total pressure losses across shock waves, present in transonic flows, are generally small, so the isentropic assumption downstream of these shocks can still be made without introducing significant errors. For the test conditions of this study, this assumption was valid. In the case of very strong shocks, the total pressure change would have to be determined by measuring the velocity vectors upstream and downstream of the shock.

As noted earlier, condensed oil vapor, already present in the flow, was used for light scattering. In a test performed on a different flow model subsequent to the subject investigations, laser velocimeter measurements were obtained across a shock wave using these oil droplets for light scattering. At the measurement station nearest the shock, a double-peaked histogram was observed, with the two peaks corresponding to the upstream and downstream velocities for the shock. The next nearest measurement stations were 1.2-mm upstream and 0.6-mm downstream from this streamwise station. At these points, the velocities measured corresponded to the respective peaks observed at the middle station. The double-peaked histogram indicated that the shock wave was not absolutely steady. However, even neglecting this unsteadiness, the distance needed for particles to attain the downstream velocity had to be less than 1.2 mm. Based on Stokes' drag law, they could not have been larger than 1-μm diam.

In the test, only the streamwise velocity component u was used to approximate the magnitude of the velocity vector. In Figs. 13a-d, typical velocity histograms obtained near the surface of the airfoil are shown. The histogram of Fig. 13a was obtained within the airfoil boundary layer, as indicated by the breadth of the histogram, which was caused by turbulent fluctuations. In Fig. 13b (a station 0.125 cm farther from the wing's surface), only a slight skewing toward lower velocities is present, indicating that the measurement station was near the edge of the boundary layer. The other two histograms of Fig. 13 were obtained outside the airfoil boundary layer; note the thinner boundary layer at the x/c = 0.4 station. Outside the boundary layer the velocity changed very gradually with increased distance from the wing's surface. Thus, measurements immediately at the boundary-layer edge were not necessary. Starting at a distance of 0.125 cm from the wing's surface, measurements were made at 0.125-cm increments until the velocity remained unchanged between stations.

The upper surface velocities obtained with the laser velocimeter, and those calculated from surface pressures at four different test conditions (α is the angle-of-attack) are shown in Figs. 14a-d. Agreement between the two sets of measurements was good for all the cases examined, even for those following a sharply-peaked velocity distribution (Fig. 14b) and downstream of a shock wave (Fig. 14d). Although there

are some differences in velocity level between the laser velocimeter and pressure measurements, the similar slopes of the velocity distributions indicate that the oil droplets were able to negotiate the changes in velocity satisfactorily. These results are indeed encouraging, and show that the laser velocimeter is a viable technique for obtaining surface pressures on two-dimensional airfoils. Additional measurements will be needed to establish ultimate accuracies and to evaluate particle trackability under the most stringent demands, such as the leading edge of the airfoil when the surface pressure is sharply peaked and at the shock location for supercritical conditions.

The laser velocimeter system employed does have the capability of making measurements from 0.5-μm diam particles, so, if the naturally occurring particles prove to be inadequate, artificial seeding with polystyrene spheres would be an alternative. A particle size of 0.5 μm should be more than adequate for inviscid flow measurements in the most severe transonic cases.

Refractive Index Effects

In neither the supersonic or transonic flows were the effects of compressibility on the index of refraction observed to present a measurement problem. Diffraction of light was observed near the shock and expansion waves in the supersonic flow, but this only required that the off-axis forward-scatter collecting optics be placed such that this scattered light did not reach the detector. The reasons why index of refraction variations did not have a noticeable effect on the measurements are believed to be the following:

1. Since θ was quite small, both incident beams experienced nearly the same index of refraction changes.

2. Wave-front distortion was minimal, since the laser beam diameters were small compared to the density scales.

3. The time over which the signal bursts occurred was short compared to the time rate of change in the density field, hence, fringe oscillation due to changing optical path length did not affect the period measurements.

CONCLUDING REMARKS

Laser velocimeter data have been presented and compared with conventional pressure-type measurements for a shock-induced separated turbulent boundary layer at a free-stream Mach number of 2.9, and for the flow over a two-dimensional airfoil section at high-subsonic and transonic conditions.

For the separated supersonic turbulent boundary layer, the laser velocimeter mean velocity determinations were found to be in good agreement with those obtained by pitot-static pressure measurements in those regions where the pressure measurements could be considered reliable. Near the wall and where the outer flow was not parallel to the probe axis agreement was not obtained; here the laser data was consistent with the physics of the flow, whereas the pressure data was not. In the realization of these measurements, no corrections were applied for any velocity biasing. These effects were believed to be unimportant, since the sampling rate was low compared to the turbulent fluctuation rate. The data were obtained using 0.5-μm diam polystyrene spheres for light scattering. Measurements across the incident shock wave showed these particles to be able to negotiate a step change in velocity in about 1 mm. Overall, the measurements are believed to be more accurate than previously obtained measurements in separated turbulent flows using physical probes.

Good agreement was obtained between laser velocimeter measurements and surface pressure data for a 6-in.-chord, two-dimensional airfoil at free-stream Mach numbers of 0.6 and 0.8. In these measurements, which were obtained from naturally occurring oil vapor droplets, particle lag effects were not evident. The measurements show that the laser velocimeter can indeed be used to determine pressure distributions on two-dimensional airfoils at transonic conditions.

REFERENCES

1. Eggins, P. L.; and Jackson, D. A.: Laser Doppler Velocity Measurements in a Supersonic Flow Without Artificial Seeding. Phys. Lett., vol. 42A, Nov. 1972, pp. 122-124.

2. Johnson, D. A.: Turbulence Measurements in a Mach 2.9 Boundary Layer Using Laser Velocimetry. AIAA Journal, vol. 12, no. 2, May 1974, pp. 711-714.

3. Yanta, W. J.; and Lee, R. E.: Determination of Turbulence Transport Properties With the Laser Doppler Velocimeter and Conventional Time-Averaged Mean Flow Measurements at Mach 3. AIAA Paper 74-575, Palo Alto, California, 1974.

4. Maurer, F.; Peterson, J. C.; Pfeifer, H. J.; and Haertig, J.: Application of a Laser-Doppler-Velocimeter in a Trans- and Supersonic Blowdown Wind Tunnel. AGARD Conference Pre-Print 174, Paper 34, Sept. 1975.

5. Johnson, D. A., and Rose, W. C.: Laser Velocimeter and Hot-Wire Anemometer Comparison in a Supersonic Boundary Layer. AIAA Journal, vol. 13, April 1975, pp. 512-515.

6. Rose, W. C.; and Johnson, D. A.: Turbulence in a Shock-Wave Boundary-Layer Interaction. AIAA Journal, vol. 13, no. 7, July 1975, pp. 884-889.

7. Abbiss, J. B.; Chubb, T. W.; and Pike, E. R.: Supersonic Flow Investigations With a Photon Correlator. Proceedings of the Second International Workshop on Laser Velocimetry, vol. I, Purdue University, Lafayette, Indiana, March 22-29, 1974.

8. Lo, C. F.: Transonic Flow Field Measurements Using a Laser Velocimeter. Proceedings of Minnesota Symposium on Laser Anemometry, Bloomington, Minnesota, Oct. 22-24, 1975.

9. Rudd, M. J.: A New Theoretical Model for the Laser Doppler Meter. J. Phys. E., series 2, vol. 2, Jan. 1969, pp. 55-58.

10. Mazumder, M. K.; and Wankum, D. L.: Signal-to-Noise Ratio and Spectral Broadening in Turbulence Structure Measurements Using a CW Laser. Appl. Opt., vol. 9, no. 3, March 1970, pp. 633-637.

11. Adrian, R. J.; and Goldstein, R. J.: Analysis of a Laser Doppler Anemometer. J. Phys. E., vol. 4, July 1971, pp. 505-511.

12. Brayton, D. B.; Kalb, H. T.; and Crossway, F. L.: A Two-Component, Dual-Scatter Laser Doppler Velocimeter With Frequency Burst Signal Readout. Project SQUID/ARMY Missile Command Workshop - The Use of the Laser Doppler Velocimeter for Flow Measurements, Purdue University, LaFayette, Indiana, March 9-10, 1972.

13. Mazumder, M. K.: Laser Doppler Velocimetry Measurement Without Directional Ambiguity by Using Frequency Shifted Incident Beams. Appl. Phys. Lett., vol. 16, no. 11, June 1970, pp. 462-464.

14. Dennison, E. B.; and Stevenson, W. H.: Oscillatory Flow Measurements With a Directionally Sensitive Laser Velocimeter. Rev. Sci. Instrum., vol. 41, no. 10, Oct. 1970, pp. 1475-1478.

15. Walsh, M. J.: Influence of Drag Coefficients Equations on Particle Motion Calculations. Proceedings of Minnesota Symposium on Laser Anemometry, Bloomington, Minnesota, Oct. 22-24, 1975.

16. Kerker, M.: The Scattering of Light and Other Electromagnetic Radiation. Academic Press, New York and London, 1969.

17. Mazumder, M. K.; Blevins, C. W.; and Kirsch, K. J.: Wind-Tunnel Flow Seeding for Laser Velocimetry Applications. Proceedings of Minnesota Symposium on Laser Anemometry, Bloomington, Minnesota, Oct. 22-24, 1975.

18. McLaughlin, D. K.; and Teiderman, W. G.: Biasing Corrections for Individual Realization of Laser Anemometer Measurements in Turbulent Flows. Phys. Fluids, vol. 16, no. 12, Dec. 1973, pp. 2082-2088.

19. Barnett, D. O.; and Bently, H. T.: Statistical Bias of Individual Realization Laser Velocimeters. Proceedings of the Second International Workshop on Laser Velocimetry, vol. I, Purdue University, LaFayette, Indiana, March 22-29, 1974.

20. Reda, D. C.; and Murphy, J. D.: Shock Wave-Turbulent Boundary-Layer Interactions in Rectangular Channels. AIAA Journal, vol. 11, Oct. 1973, pp. 1367-1368.

TABLE 1 - PARTICLE RESPONSE BASED ON STOKES' DRAG LAW FOR $M_\infty = 2.9$, $T_t = 293°K$, AND PARTICLES WITH A SPECIFIC GRAVITY OF 1.

d_p (μm)	τ_c (μsec)	f_{3dB} (kHz)	x_c (mm)
2	30	5	18
1	7.4	21	4.5
0.5	1.9	85	1.1
0.3	0.7	286	0.4

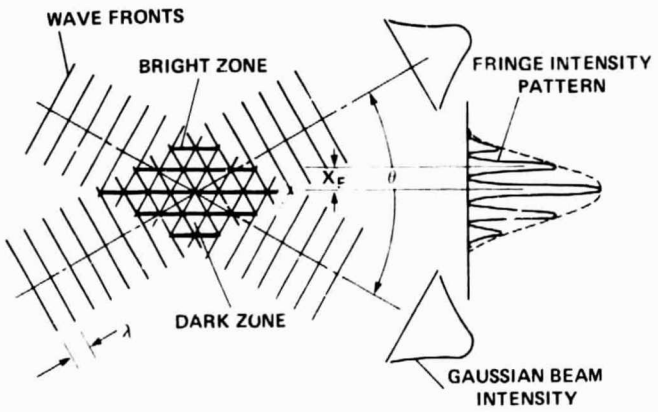

Fig. 1 Intensity fringes formed at beam crossover.

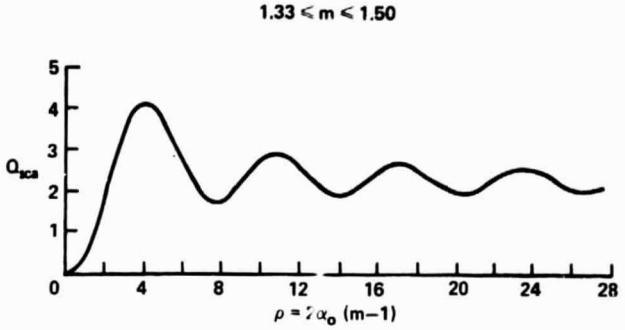

Fig. 2 Scattering efficiency, Q_{sca}, plotted against the parameter $\rho = 2\alpha_o (m - 1)$ (from Ref. 16).

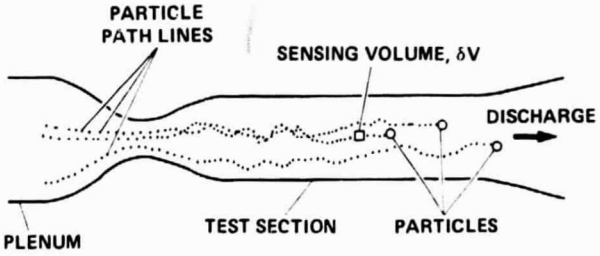

Fig. 3 Particle passage through flow facility and sensing volume δV.

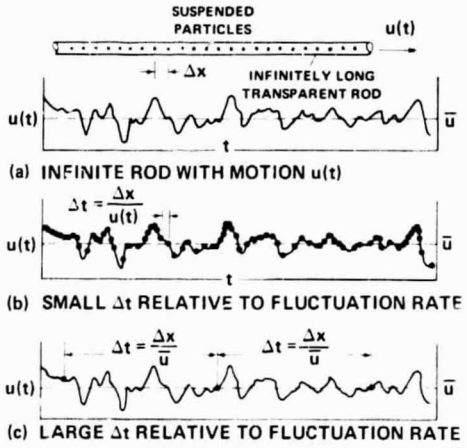

Fig. 4 One-dimensional analogy for velocity bias.

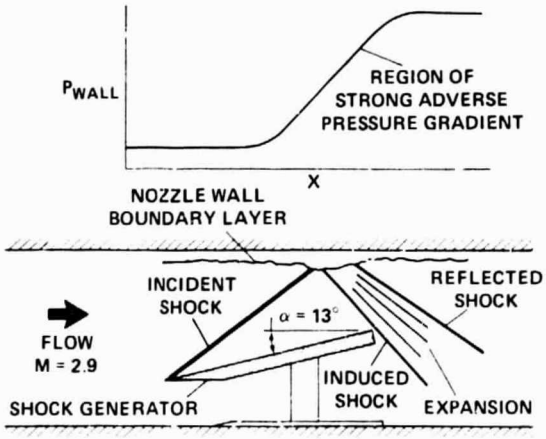

Fig. 5 Flow model for shock-induced separation.

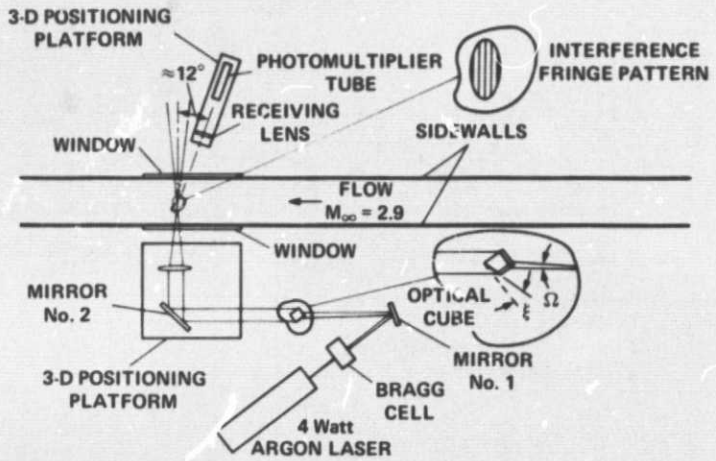

Fig. 6 Laser velocimeter system: Ames 8- by 8-Inch Supersonic Wind Tunnel.

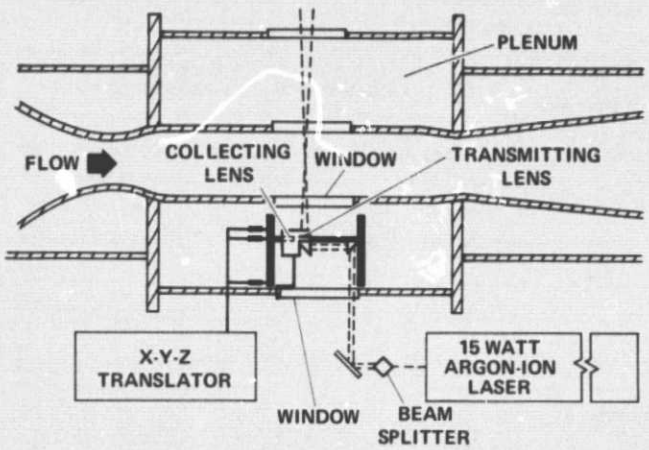

Fig. 7 Laser velocimeter system: Ames 2- by 2-Foot Transonic Wind Tunnel.

Fig. 8 Photograph of scanning portion of laser velocimeter.

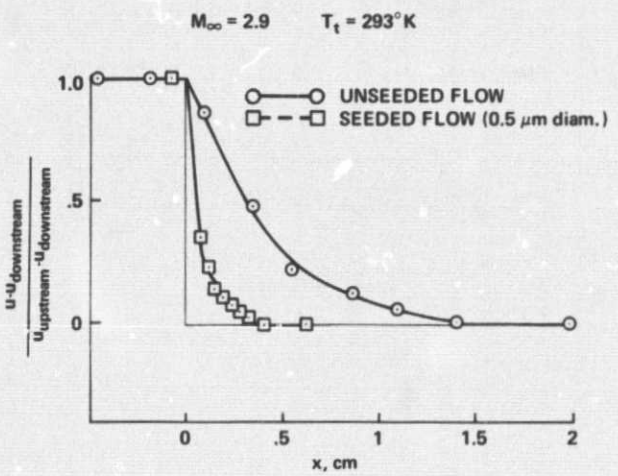

Fig. 9 Particle response to oblique shock wave at $M_\infty = 2.9$.

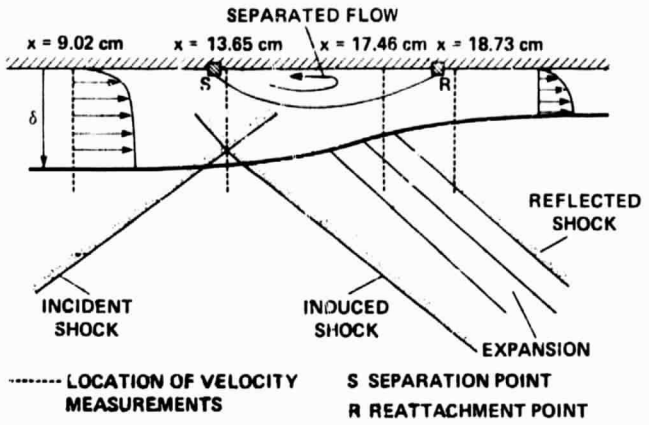

Fig. 10 Representation of flow field generated by 13° wedge.

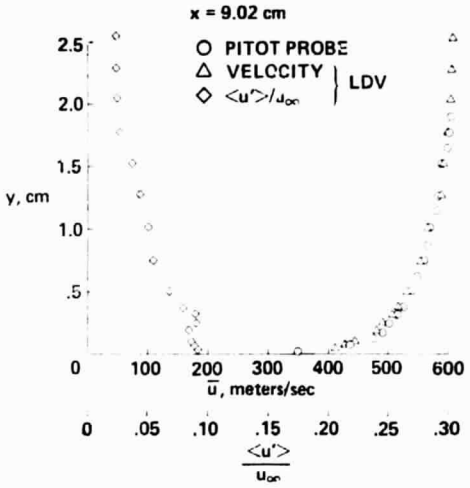

(a) Upstream of interaction.

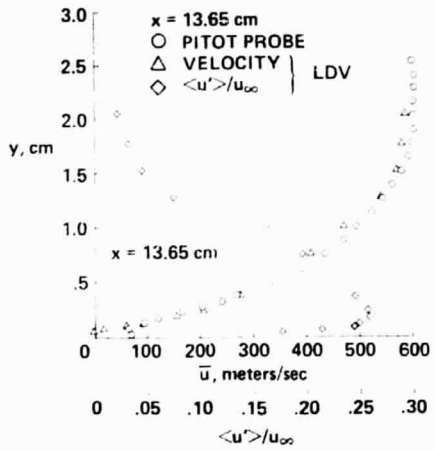

(b) Near separation point.

Fig. 11 Mean velocity and turbulence intensity profiles.

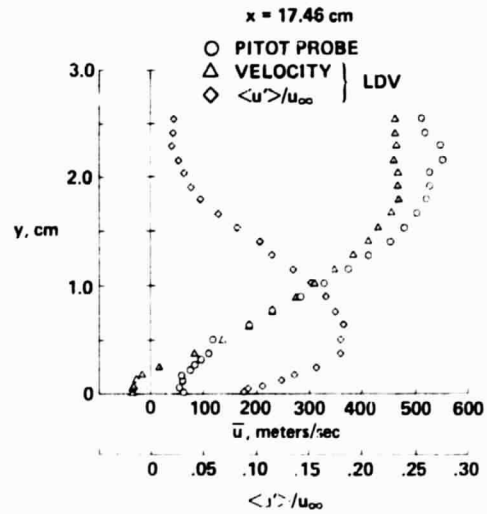

(a) Within separated region.

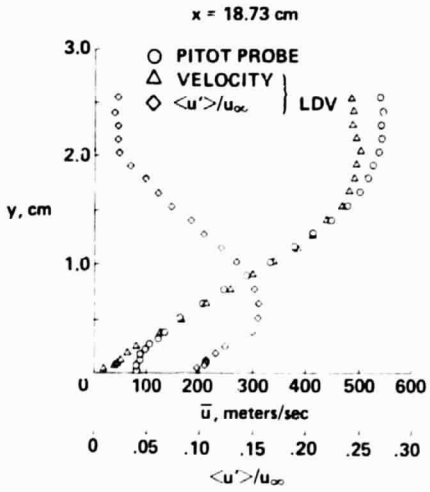

(b) Near reattachment point.

Fig. 12 Mean velocity and turbulence intensity profiles.

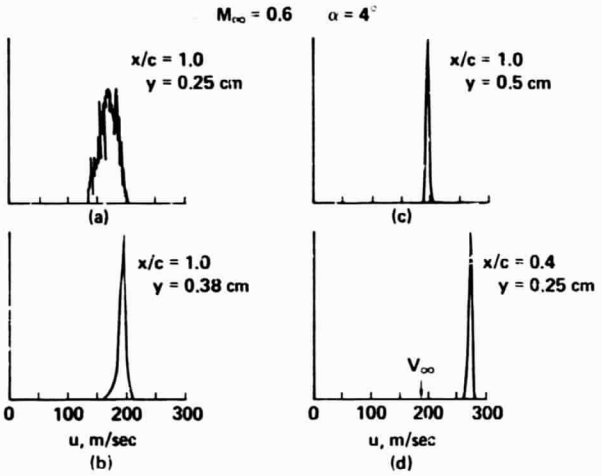

Fig. 13 Velocity histograms - NACA 64A010 airfoil at M_∞ = 0.6 and α = 4°.

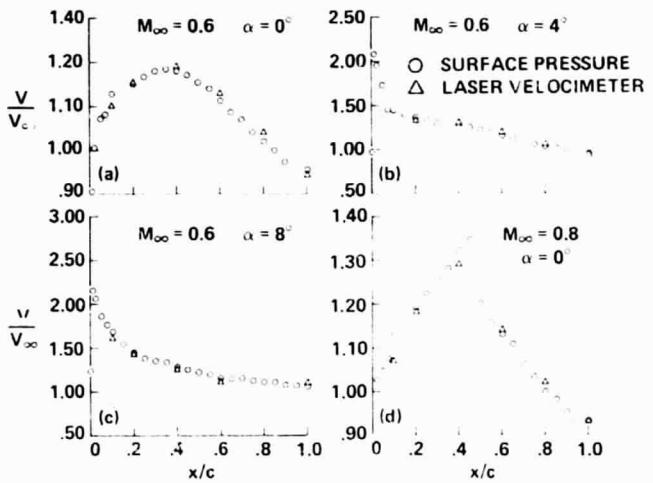

Fig. 14 Velocity comparison - upper surface NACA 64A010 airfoil.